Bioorganic Chemistry 110 (2021) 104825

Contents lists available at ScienceDirect

Bioorganic Chemistry

journal homepage: www.elsevier.com/locate/bioorg

Discovery of novel quinazoline-based covalent inhibitors of KRAS G12C with various cysteine-targeting warheads as potential anticancer agents

Ling Li, Huiting Zhao, Hui Liao, Jingxuan Chen, Jin Liu, Jianjun Chen *

School of Pharmaceutical Sciences, Guangdong Provincial Key Laboratory of New Drug Screening, Southern Medical University, Guangzhou 510515, China

ARTICLE INFO

Keywords:
KRAS G12C
Covalent inhibitors
Anticancer
Cysteine-targeting warheads

ABSTRACT

A series of novel quinazoline analogs with a variety of cysteine-targeting warheads (electrophiles) were designed and synthesized based on ARS-1620 as covalent KRAS G12C inhibitors. Among them, compounds **LLK10** and **LLK14** exhibited similar or better antiproliferative activity than ARS-1620. **LLK10** was used for subsequent biological studies due to the higher selectivity towards KRAS G12C-mutated cells than **LLK14**. **LLK10** maintained the mechanism of action by forming a covalent bond with KRAS G12C protein, thus decreasing the level of phosphorylated Mek and Erk, and leading to tumor cell apoptosis. In addition, **LLK10** was able to suppress the formation of H358 tumor colonies. Molecular modeling study indicated that **LLK10** binds with high affinity to the SWII binding site in KRAS G12C and overlaps well with ARS-1620. The high binding affinity of **LLK10** was further confirmed by the isothermal titration calorimetry (ITC) assay in which **LLK10** exhibited a K_D of 115 nM for binding to KRAS G12C. These results suggest that the novel covalent inhibitors of KRAS G12C with different warheads deserve further investigation as potential anticancer agents.

1. Introduction

RAS proteins are GTPases controlling the activity of several critical signaling pathways that regulate cell differentiation, proliferation, and survival [1,2]. RAS gene family comprises three members (KRAS, HRAS, and NRAS), which function as a binary switch transitioning between the active (GTP-bound) state and the inactive (GDP-bound) state [3]. Mutated RAS is constitutively activated and constantly turned "on", thus resulting in accretion of GTP-bound activated RAS and activation of downstream signaling pathways (e.g. RAS-Raf-Mek-Erk), eventually leading to the development of cancer (Fig. 1) [4]. KRAS is the most frequently mutated oncogene in human cancer, occurring in 30% of human tumors. Among KRAS mutant tumors, 80% of all oncogenic mutations occur within codon 12, especially p.G12C, where glycine was substituted by cysteine residue [5].

Although KRAS mutations are common in a large number of cancer patients, to date, there is no effective therapy that specifically targets mutant KRAS available in clinic, despite the intensive efforts made by researchers [6]. KRAS is conventionally deemed "undruggable" due to the extremely high binding affinity (picomolar) to GDP and GTP within the cells, along with the high micromolar concentrations of intracellular GTP (~500 μM) [3], making it unlikely that a drug molecule would be able to compete for binding to the GTP-site of KRAS. Additionally, the absence of deep and hydrophobic binding pockets on the surface of oncogenic KRAS protein also hindered the discovery of effective inhibitor molecules. Furthermore, KRAS activation and signaling is accomplished through protein–protein interactions (PPIs), which are challenging to target because of the relatively featureless and flat to pologies of the surfaces involved [7].

In 2013, Shokat and co-workers reported a novel strategy to target the reactive cysteine 12 (Cys12) of KRAS G12C using covalent inhibitors [8]. They proposed that covalently modifying Cys12 could disrupt KRAS G12C-driven signaling pathway by forming a covalent bond between the inhibitor and Cys12 of KRASG12C. They developed a series covalent inhibitors (e.g.ARS-1620 and ARS-917, Fig. 2A), which covalently bound to Cys12 of the GDP-bound form of KRAS, with the quinazoline core of the molecule occupying an allosteric pocket (the "switch II pocket" (S-IIP)) (Fig. 2B) [9].

Recently, there has been a growing interest in the development of irreversible and reversible covalent inhibitors targeting the catalytic or noncatalytic amino acids (e.g. cysteine) of KRAS [10]. In an effort to identify more effective and selective KRAS G12C inhibitors for cancer treatment, we designed a series of quinazoline-based molecules (**LLK1-14**) by varying the covalent warheads (the electrophiles) of ARS-1620

* Corresponding author.
E-mail address: jchen21@smu.edu.cn (J. Chen).

https://doi.org/10.1016/j.bioorg.2021.104825
Received 16 January 2021; Received in revised form 3 March 2021; Accepted 9 March 2021
Available online 13 March 2021

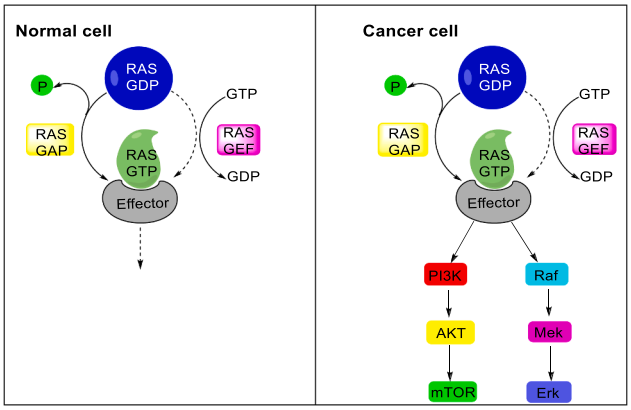

Fig. 1. Overview of Ras signaling pathway. The mutation of RAS activates the protein into a hyperexcitable state, thus resulting in accretion of GTP-bound activated RAS and activation of downstream signaling pathways.

(Fig. 3), and explored the impact of different electrophilic warheads on the activity. Herein, we report the design, synthesis, and biological activities of these covalent inhibitors of KRAS G12C.

2. Results and discussion

2.1. Chemistry

The synthesis of target compounds **LLK1 ~ 14** is outlined in Scheme 1. To a solution of 7-bromo-6-chloroquinazolin-4-ol in thionyl chloride, DMF was added and the resulting mixture was stirred at 80 °C for 8 h to obtain the chlorinated compound **2**. Then, to a solution of compound **2** in DMF at 0 °C, DIPEA and tert-butyl piperazine-1-carboxylate were added, and the resulting mixture was stirred at 50 °C for 2 h to generate compound **3** via nucleophilic substitution. Compound **3** was subjected to a Suzuki reaction with 2-fluoro phenyl boronic acid to produce the quinazoline intermediate **4**. Removal of the Boc-group from intermediate **4** under acidic conditions yielded compound **5**, which was coupled with various carboxylic acids using (Benzotriazol-1-yloxy) tris(dimethylamino) phosphonium hexafluorophosphate (BOP) as the coupling reagent to give compound **6** (**LLK12**), or compounds **LLK10 ~ 14**. Compounds **LLK1 ~ 9** were synthesized by reacting compound **6** (**LLK12**) with different aldehydes under basic conditions.

2.2. Biological evaluations

2.2.1. In vitro antiproliferative activity and structure–activity relationship

The antiproliferative activities of the newly synthesized compounds (**LLK1-14**) against five human cancer cell lines were evaluated by using the standard MTT assay with ARS-1620 as positive control. As shown in Table 1, compounds **LLK1** to **LLK6** with an electron donating substituent on the double bond (covalent warhead) showed low antiproliferative activity on KRAS G12C mutated cancer cell lines (Miapanc2, H358), with IC_{50} values of >30 μM. However, compounds with an electron withdrawing group on the double bond, for example, **LLK7-10** and **LLK14**, displayed improved antiproliferative activities with IC_{50} values in the low to medium micromolar range (1.20–25.1 μM). Among them, **LLK10** and **LLK14** exhibited the highest antiproliferative potency with IC_{50} values of 4.06 μM and 1.50 μM against Miapanc2 (KRAS G12C) cells, and 2.34 μM and 1.20 μM against H358 (KRAS G12C) cells, respectively, similar to that of ARS-1620 (IC_{50} = 2.81 and 0.18 μM for Miapanc2 and H358 cells, respectively). Notably, the activity of **LLK14** in Miapanc2 cells (IC_{50} = 1.50 μM) is better than that of ARS-1620 (IC_{50} = 2.81 μM). In addition, compound **LLK10** demonstrated good selectivity towards KRAS G12C-mutated H358 cells (IC_{50} = 2.34 μM) over KRAS G12S-mutated A549 (IC_{50} = 8.60 μM) and KRAS G12D-mutated Panc1 cells (IC_{50} = 7.34 μM) as well as the wild-type MCF7 cells (IC_{50} = 7.48 μM). However, for compounds with the unsaturated bond (electrophilic warhead) replaced by a saturated bond (**LLK11** and **LLK12**), a complete loss of activity was observed (e.g. IC_{50} > 50 μM), indicating that the unsaturated bond (electrophilic warhead) is critical for activity. Based on the high antiproliferative activity and good selectivity towards KRAS G12C-mutated cancer cells, **LLK10** was selected for subsequent biological studies as detailed below.

2.2.2. Colony formation assay

Colony formation assay has been widely utilized for prediction of *in vivo* antitumor efficacy of a drug molecule [11]. To further validate the *in vitro* antiproliferative activities of the newly synthesized compounds, we evaluated the ability of one of the best compounds, **LLK10** (IC_{50} = 2.34 μM, Fig. 4A) to inhibit H358 tumor colony formation at five different concentrations (2 μM, 4 μM, 6 μM, 8 μM, 10 μM). As shown in Fig. 4B, **LLK10** was able to suppress the formation of H358 tumor colonies in a dose-dependent manner, with the colony-forming ability of H358 cells being totally suppressed after 24 h treatment with 2 μM of **LLK10.**

2.2.3. LLK10 covalently bound to KRAS G12C

To determine whether compound **LLK10** maintained the mechanism of action by forming a covalent bond with KRAS G12C, we incubated

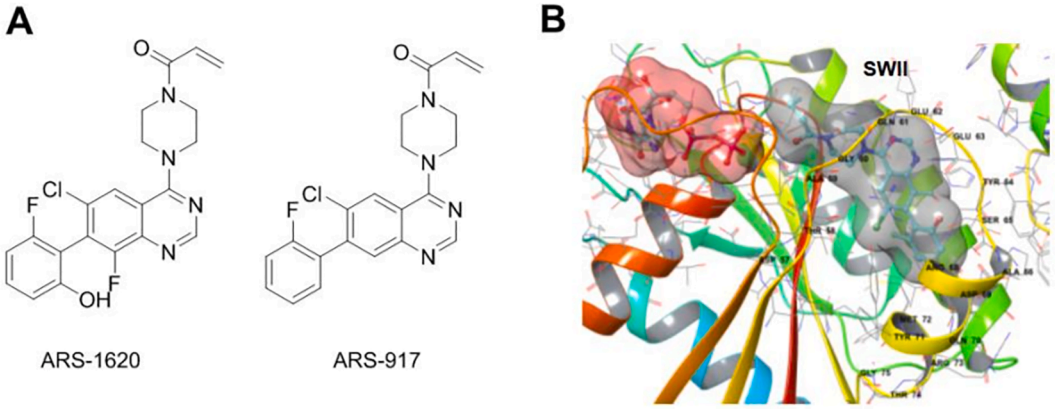

Fig. 2. A: The chemical structures of ARS-1620 and ARS-917; B: The crystal structure of ARS-1620 in complex with KRAS G12C (PDB code: **5V9U**). The gray part represents ARS-1620. The pink part represents GTP. (For interpretation of the references to colour in this figure legend, the reader is referred to the web version of this article.)

KRAS G12C protein with **LLK10** and observed the expected mass gain (MS = 464) using mass spectrometry (Fig. 5A to F). This result indicated that **LLK10** binds through a covalent bond to KRAS G12C protein.

2.2.4. LLK10 exhibited high binding affinity to KRAS G12C protein

To further confirm whether the KRAS G12C inhibitor **LLK10** can bind to KRAS G12C, we assessed its binding affinity to KRAS G12C by using isothermal titration calorimetry (ITC) and circular-dichroism spectroscopy (CD) analysis. As shown in Fig. 6A, **LLK10** exhibited high binding affinity to KRAS G12C with a K_D of 115 nM. Moreover, CD spectroscopy also indicated that the conformation of secondary structures of KRAS G12C protein changed when **LLK10** was mixed with KRAS G12C (Fig. 6B), as compare to the control (KRAS G12C protein only). Collectively, these results (ITC and CD) suggest that **LLK10** binds to KRAS G12C protein with high binding affinity.

2.2.5. LLK10 modulates Erk signaling in KRAS G12C mutant cell lines

To explore the mechanism of action for these newly synthesized compounds, **LLK10** was selected for evaluation of the effects on the downstream signaling pathway (e.g. MeK, Erk) of KRAS by western blot analysis. As shown in Fig. 7A and C, **LLK10** decreased the levels of pMek and pErk (phosphorylated Mek and Erk) at a concentration of 10 μM. However, the levels of pMek and pErk rebound at a concentration of 15 μM. This may because the negative feedback of RAS signaling. In addition, **LLK10** didn't alter the level of KRAS but decreased the level of phosphorylated Mek and Erk in a time-dependent manner at 10 μM (Fig. 7B and D). These results are consistent with literature reports for the mechanism of action of ARS-series of compounds.[9]

2.3. Molecular modeling study for LLK10 with KRAS G12C protein

To better understand how the compounds interact with KRASG12C, covalent molecular docking simulation of **LLK10** and ARS-1620 at the SWII site in the KRASG12C was investigated using the covalent docking protocol in the Schrodinger 2011 molecular modeling suite (Schrodinger, Inc., New York, NY) and the KRAS crystal structure (PDB code: **5V9U**). The 3D model of **LLK10** and ARS-1620 (Fig. 8A) showed that **LLK10** fitted nicely to the SWII site and overlapped well with ARS-1620 in the same pocket. Two hydrogen bonds were formed between the pyrimidine ring and HIS95, carbonyl and LYS16 (Fig. 8B). The π-π interaction between the pyrimidine ring and TYR 96 was also observed. Collectively, these binding interaction may explain the high activity of **LLK10** against KRAS G12C mutated cells.

3. Conclusion

In summary, a series of novel quinazolines analog with different electrophilic warheads were designed and synthesized based on ARS-1620 as covalent KRAS G12C inhibitors and a focused SAR study was conducted. These compounds exhibited high antiproliferative potency against KRAS G12C mutated cancer cell lines with IC_{50} values at low micromolar levels. Structure-activity relationships revealed that the substituents on the acrylamide have great influence on the biological activities of the compounds (e.g. electron withdrawing groups are more favorable). Among the newly synthesized compounds, **LLK10** and **LLK14** were identified as two of the most potent compounds against KRAS G12C mutated cancer cells, with the activity being similar or better than that of ARS-1620. **LLK10** showed higher selectivity than **LLK14** and was chosen for subsequent biological studies. **LLK10** demonstrated high inhibitory activity against H358 tumor colony formation. Mass spectrometry, CD, and ITC studies indicated that **LLK10** binds covalently to KRASG12C protein with high affinity (K_D of 115 nM by ITC) and changed the conformation of secondary structures of KRAS G12C protein. In addition, western blot analysis revealed that **LLK10** decreased the levels of phosphorylated Mek and Erk, similar to ARS-series of compounds. Molecular docking study suggested that **LLK10** binds well to and overlaps nicely with ARS-1620 in the SWII binding pocket of KRAS G12C protein. These results suggest that **LLK10**, with the novel acrylamide warhead for covalent binding, may serve as a starting point for developing more effective KRAS G12C inhibitors for cancer treatment.

4. Experimental section

4.1. Chemistry

Unless otherwise specified, all materials were obtained from commercial sources and used without purification. The reference compound ARS-1620 was purchased from InvivoChem (Libertyville, IL 60048, USA). Reaction time and purity of the products were determined by thin-layer chromatography (TLC) with fluorescent indicator visualizable at 254 nm and 365 nm. Column chromatography was performed on silica gel (100–200 mesh). ^{1}H NMR (400 MHz) spectra and ^{13}C NMR (101 MHz) spectra were recorded on a Bruker Avance 400 MHz NMR spectrometer with $CDCl_3$ as the solvent.

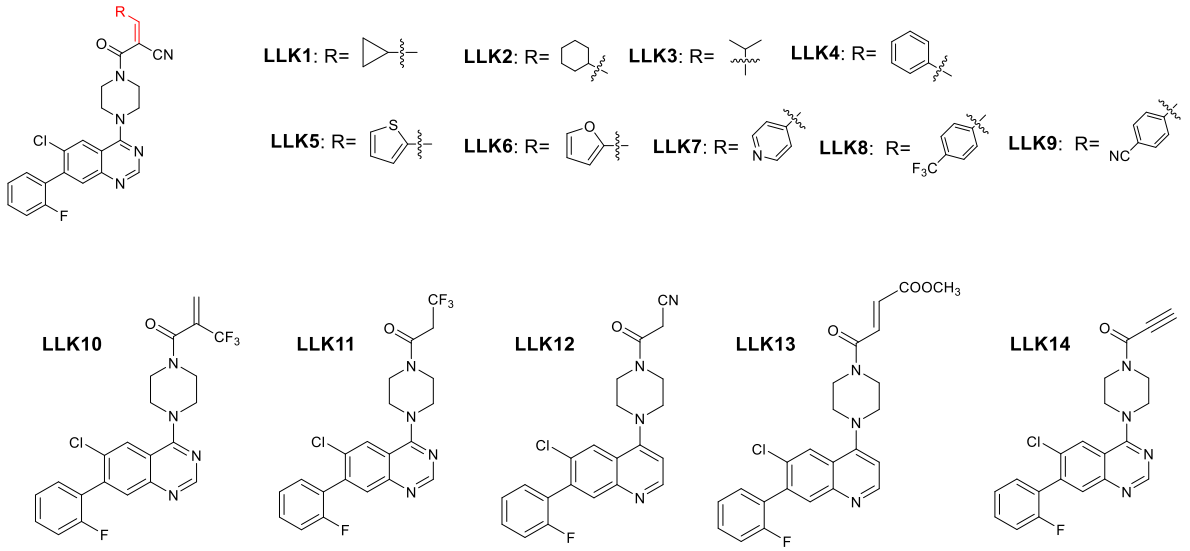

Fig. 3. Design of ARS-1620-based covalent inhibitors of KRAS G12C bearing different electrophilic warheads.

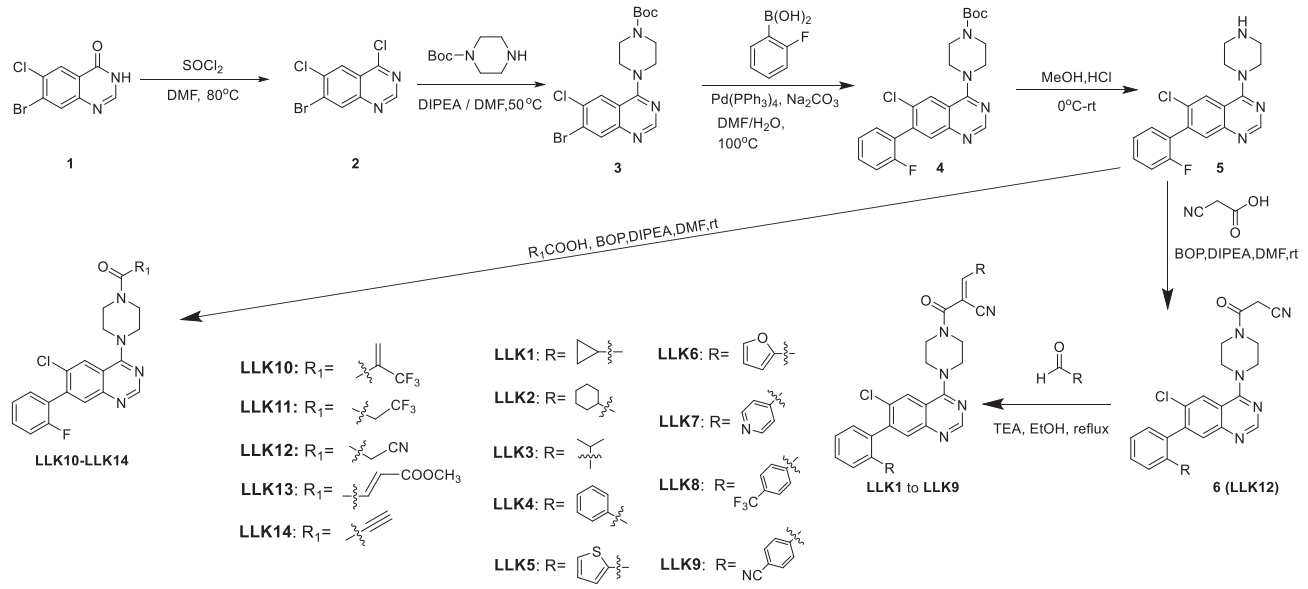

Scheme 1. Synthesis of compounds **LLK1-14.**

Table1
In vitro antiproliferative activity of compounds **LLK1-14.**

Structure	ID	R	IC_{50}(μM)				
			Pancreatic cancer Miapanc2 (G12C)	Lung cancer H358(G12C)	Pancreatic cancer Panc1(G12D)	Lungcancer A549(G12S)	Breast cancer MCF7 (WT)
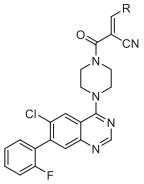	**LLK1**		>30	>30	>50	>50	>50
	LLK2		31.17 ± 4.72	>30	>50	>50	>50
	LLK3		>30	>30	>50	>50	>50
	LLK4		>30	>30	>50	>50	>50
	LLK5		>30	>30	>50	>50	>50
	LLK6		56.98 ± 4.83	>30	>50	>50	>50
	LLK7		25.11 ± 0.01	>10	>50	>50	>50
	LLK8		18.61 ± 1.26	22.41 ± 1.74	33.24 ± 0.36	>50	>50
	LLK9	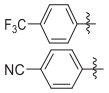	14.78 ± 0.45	18.59 ± 0.36	>50	>50	>50
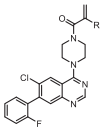	**LLK10**	CF_3	4.06 ± 0.91	2.34 ± 0.917	7.34 ± 0.20	8.60 ± 1.33	7.48 ± 1.19
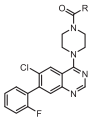	**LLK11**	CH_2CF_3	>10	>10	>50	>50	>50
	LLK12	CH_2CN	>10	>10	>50	>50	>50
	LLK13	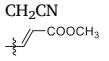	>10	>10	>50	>50	>50
	LLK14		1.50 ± 0.20	1.20 ± 0.412	2.31 ± 0.53	3.71 ± 0.06	7.10 ± 0.54
	ARS-1620		2.81 ± 0.99	0.18 ± 0.073	38.86 ± 2.48	38.86 ± 4.70	>100

4.1.1. General procedure for preparation of compounds 2

To a solution of 7-bromo-6-chloroquinazolin-4-ol (2600 mg, 10 mmol) in thionyl chloride (80 mL), one drop of N,*N*-dimethylformamide was added and the resulting mixture was stirred at reflux for 8 h. The mixture was allowed to cool to room temperature and concentrated *in vacuo* to afford the crude product. The crude product was used directly in the next step without purification.

4.1.2. General procedure for preparation of compounds 3

To a solution of7-bromo-4,6-dichloroquinazoline (2780 mg, 10 mmol) in dichloromethane (100 mL) at 0 °C, N,*N*-Diisopropylethylamine (3900 mg, 30 mmol) and tert-butyl piperazine-1-carboxylate (1860 mg, 10 mmol) were added and the resulting mixture was stirred at 50 °C for 2 h. The mixture was allowed to cool to room temperature and added water to separate out compound.

4.1.3. General procedure for preparation of compounds 4

To a solution of tert-butyl 4-(7-bromo-6-chloroquinazolin-4-yl) piperazine-1-carboxylate (1500 mg, 3.5 mmol) and 2-fluorophenylboronic Acid (980 mg, 7 mmol) in 1,4-dioxane (60 mL) and water (20

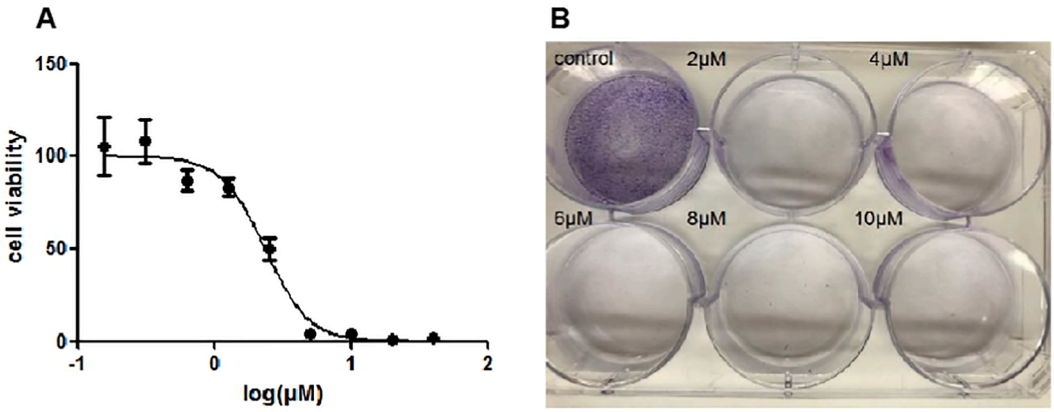

Fig. 4. **LLK10** suppressed the formation of H358 tumor colonies. A: Antiproliferative activity of **LLK10** against H358 cancer cells; B: Inhibition of H358 tumor colony formation by **LLK10**.

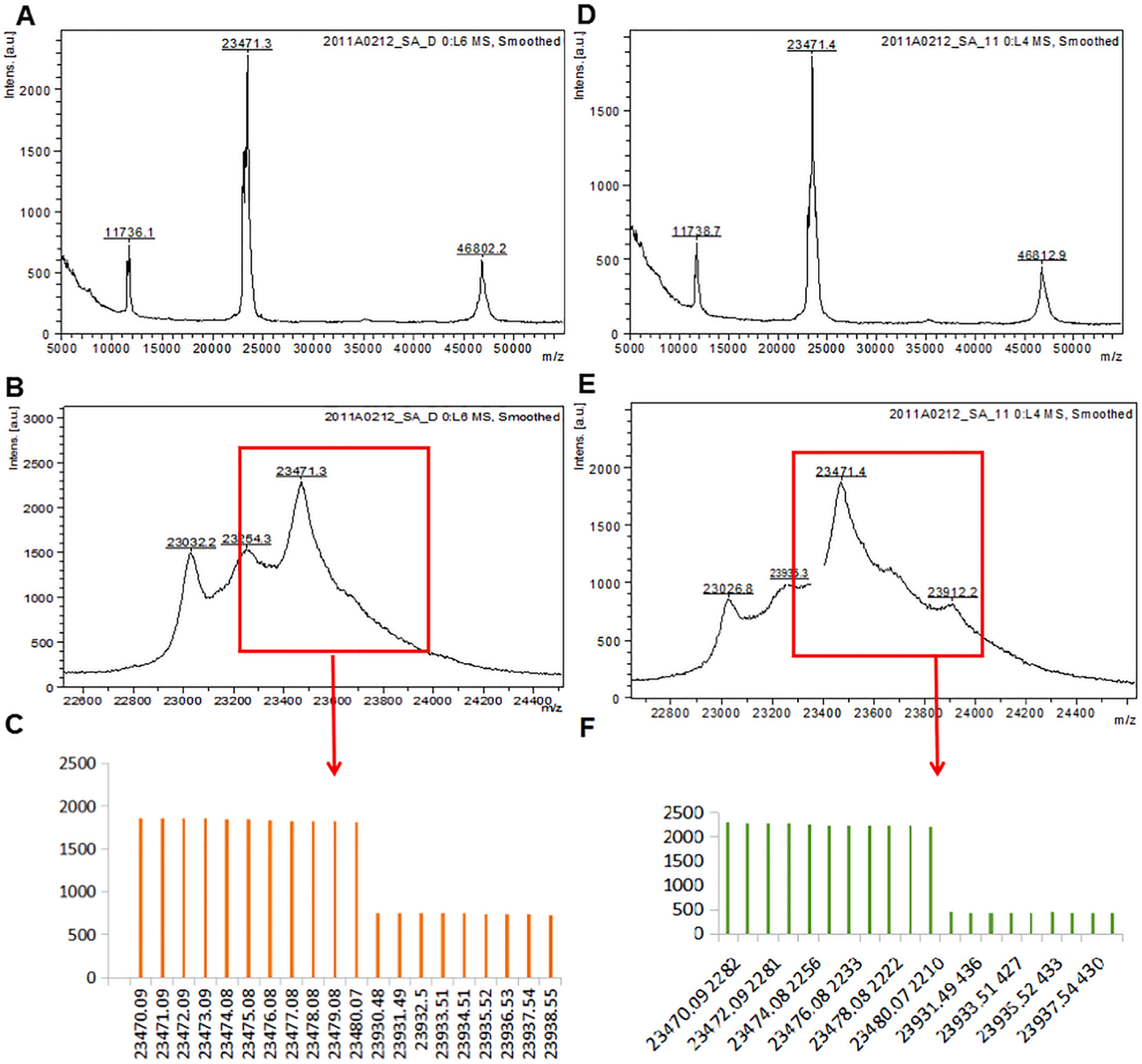

Fig. 5. **LLK10** bound covalently to KRAS G12C protein. Mass spectrometry (MS analysis) confirms covalent labeling of **LLK10** with KRAS-G12C. After incubation of protein with DMSO (A to C) or **LLK10** (D to F), reactions were resolved by LC-MS. The mass spectra revealed a shift in protein mass corresponding to **LLK10**.

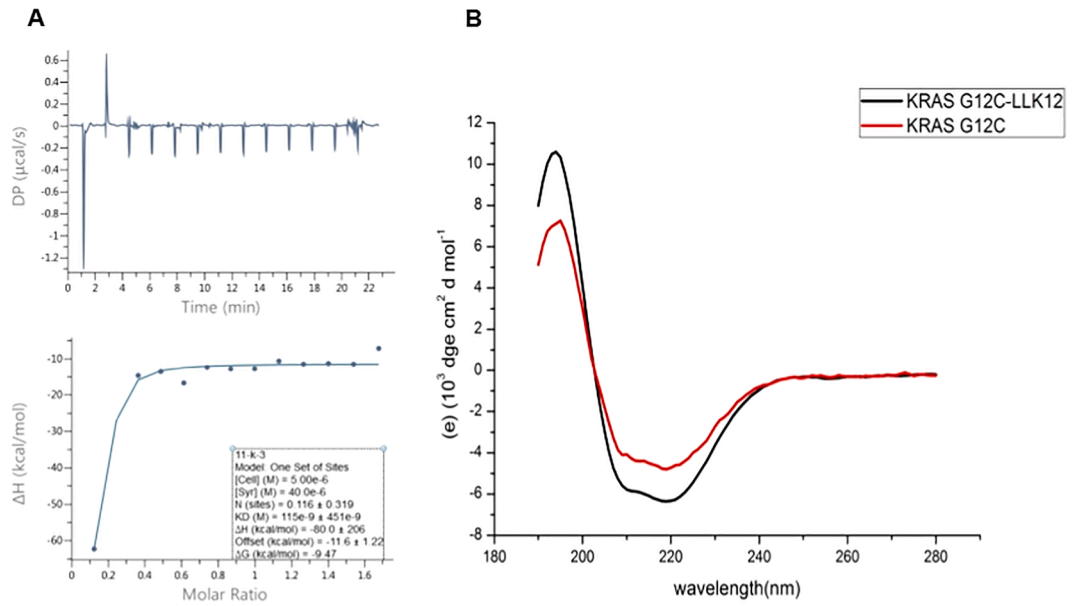

Fig. 6. A: The binding affinity of **LLK10** to KRAS G12C as measured by ITC; B: Circular dichroism spectra of KRAS G12C in complex with **LLK10.**

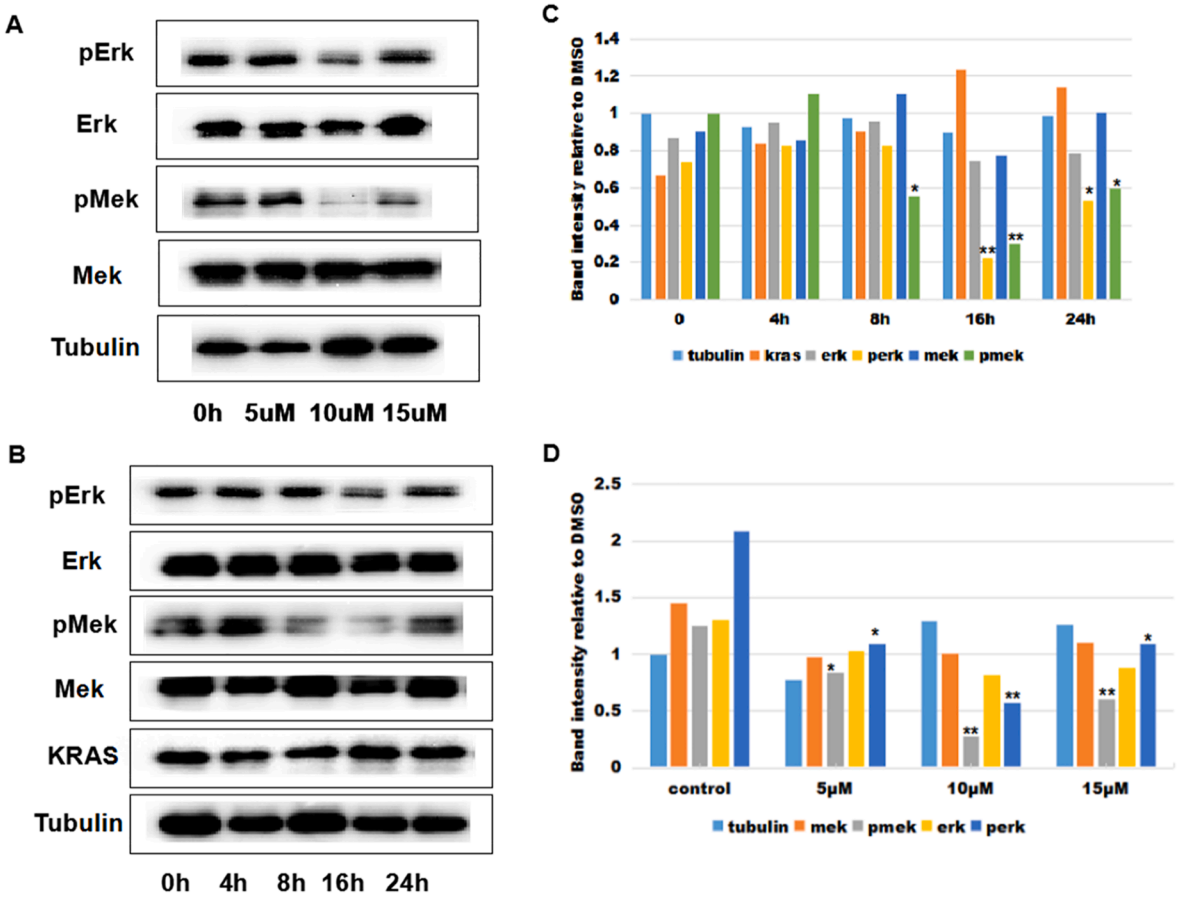

Fig. 7. LLK10 modulates Erk signaling in H358 cancer cells. Each data point represents three independent experiments, *P < 0.05, **P < 0.01.

mL) under argon atmosphere, $Pd(PPh_3)_4$ (400 mg, 0.35 mmol) and Na_2CO_3 (1110 mg, 10.5 mmol) were added and the resulting mixture was stirred at 100 °C for 24 h. The mixture was allowed to cool to room temperature and concentrated *in vacuo*. The residue was purified by flash column chromatography on silica gel to afford the desired product.

4.1.4. General procedure for preparation of compounds 5

To a solution oftert-butyl 4-(6-chloro-7-(2-fluorophenyl)quinazolin-4-yl)piperazine-1-carboxylate (880 mg, 2 mmol) in dichloromethane (20 mL) at room temperature, HCl in MeOH (100 mL) was added and the resulting mixture was stirred at room temperature for 1 h. The mixture was concentrated *in vacuo.*

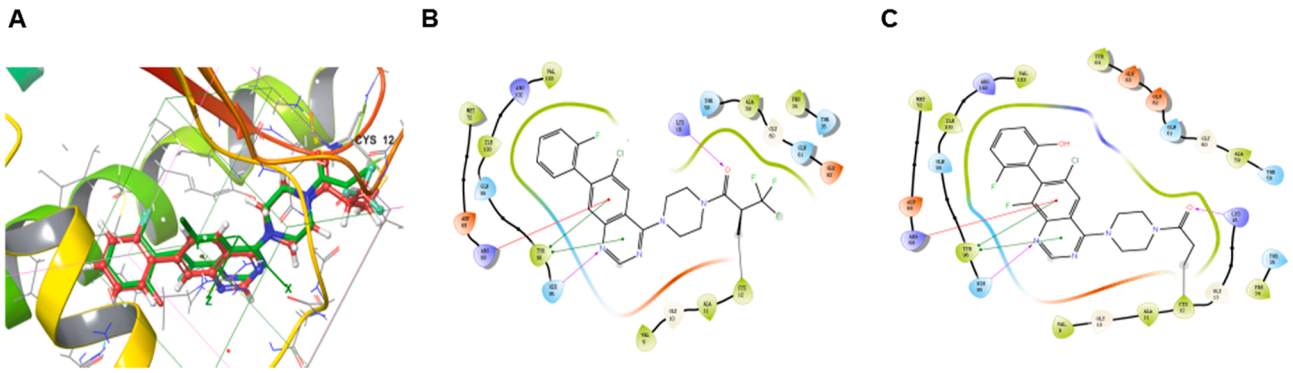

Fig. 8. The 3D model of **LLK10** and ARS-1620 in SWII site (A) the red stick model represents ARS-1620, the green stick model represents **LLK10.** The 2D model of **LLK10** (B) and ARS-1620 (C). (For interpretation of the references to colour in this figure legend, the reader is referred to the web version of this article.)

4.1.5. General procedure for preparation of compounds LLK10-LLK14

To a solution of compound **5** (36.8 mg, 0.1 mmol) in DMF was added TEA (20 mg, 0.2 mmol) , BOP (88 mg, 0.2 mmol) and substituted carboxylic acid acid (0.1 mmol) and stirred overnight. The reaction mixture was added water and then purified by flash column chromatography on silica gel and HPLC to afford the desired product.

4.1.6. General procedure for preparation of compounds LLK1 to LLK9

To a solution of compound **6** (40 mg, 0.1 mmol) in EtOH was added TEA (0.2 mmol), fatty aldehyde or aromatic aldehyde (0.1 mmol) was added and stirred at 50 °C overnight. The mixture was concentrated *invacuo*. The residue was purified by flash column chromatography on silica gel and HPLC to afford the desired product.

4.1.6.1. tert-butyl 4-(7-bromo-6-chloroquinazolin-4-yl)piperazine-1-carboxylate (3). White solid. Yield: 80%. ^{1}H NMR (400 MHz, $CDCl_3$) δ = 8.877 (s, 1H), 7.810 (s, 1H), 7.805 (s, 1H), 3.80–3.82 (m, 4H), 3.65–0.368 (m, 4H), 1.519 (s, 9H).

*4.1.6.2. tert-butyl 4-(6-chloro-7-(2-fluorophenyl)quinazolin-4-yl)piperazine-1- carboxy late (**4**).* White solid. Yield: 80%. ^{1}H NMR (400 MHz, CDCl3): δ8.786 (s, 1H), 8.011 (s, 1H), 7.930 (s, 1H), 7.479–7.515 (m, 1H), 7.412–7.479 (m, 1H), 7.298–7.394 (m, 1H), 7.207–7.286 (m, 1H), 3.816–3.839 (m, 4H), 3.690–3.714 (m, 4H), 1.533 (s, 9H).

*4.1.6.3. 1- (4-(6-chloro-7-(2-fluorophenyl)quinazolin-4-yl)piperazin-1-yl) prop-2-en-1-one(**5**).* White oil. Yield: 80%. ^{1}H NMR (400 MHz, DMSO): δ 8.909 (s, 1H), 8.836(s, 1H), 7.979 (s, 1H), 7.623–7.718 (m, 1H), 7.525–7.607 (m, 1H), 7.449–7.507 (m, 1H), 7.395–7.430 (m, 1H), 4.227 (m, 8H).

4.1.6.4. (4-(6-chloro-7-(2-fluorophenyl)quinazolin-4-yl)piperazine-1-carbonyl)-3-cyclopropylacrylonitrile (LLK-1). White oil. Yield: 1%. 1H NMR (400 MHz, $CDCl_3$) δ = 8.78 (s, 1H), 8.00 (s, 1H), 7.93 (s, 1H), 7.51–7.42 (m, 1H), 7.41–7.34 (m, 1H), 7.29 (d, J = 7.4 Hz, 1H), 7.24–7.19 (m, 1H), 6.70 (d, J = 11.2 Hz, 1H), 3.98–3.80 (m, 8H), 2.18–2.07 (m, 1H), 1.34–1.26 (m, 2H), 0.97–0.90 (m, 2H). HRMS calculated for $C_{25}H_{21}ClFN_5$ $[M+H]^+$462.1497. found 462.1495. Purity: 96.34% by HPLC (t_R = 17.393 min, 17.586 min).

4.1.6.5. 2-(4-(6-chloro-7-(2-fluorophenyl)quinazolin-4-yl)piperazine-1-carbonyl)-3-cyclohexylacrylonitrile (LLK-2). Yellow oil. Yield: 6%. ^{1}H NMR (400 MHz, $CDCl_3$) δ = 8.79 (s, 1H), 7.99 (s, 1H), 7.93 (s, 1H), 7.50–7.44 (m, 1H), 7.37 (t, J = 5.7 Hz, 1H), 7.29 (d, J = 7.5 Hz, 1H), 7.23–7.18 (m, 1H), 7.05 (d, J = 10.3 Hz, 1H), 4.05–3.75 (m, 8H), 2.74–2.66 (m, 1H), 1.47–1.22 (m,10*H*). HRMS calculated for $C_{28}H_{27}ClFN_5O$ $[M+H]^+$ 504.1966. found 504.1967. Purity: 99.15% by HPLC (t_R = 17.467 min, 17.406 min).

4.1.6.6. 2-(4-(6-chloro-7-(2-fluorophenyl)quinazolin-4-yl)piperazine-1-carbonyl)-4-methylpent-2-enenitrile (LLK-3). Yellow oil. Yield: 1%. ^{1}H NMR (400 MHz, $CDCl_3$) δ = 8.79 (s, 1H), 7.99 (s, 1H), 7.93 (s, 1H), 7.51–7.44 (m, 1H), 7.38 (t, J = 7.4 Hz, 1H), 7.29 (d, J = 7.5 Hz, 1H),7.24–7.18 (m, 1H), 7.04 (d, J = 10.3 Hz, 1H), 3.94–3.81 (m, 8H), 3.04–2.97 (m, 1H), 1.18 (d, J = 6.5 Hz, 6H).^{13}C NMR (101 MHz, $CDCl_3$) δ166.90, 163.28, 162.53, 158.25, 154.38, 140.34, 131.61, 131.35, 131.20, 131.17, 130.73, 130.65, 124.60, 124.17, 115.88, 115.66, 115.40, 106.99, 49.23, 15.73, 10.86. HRMS calculated for $C_{25}H_{23}ClFN_5O$ $[M+H]^+$ 464.1653. found 464.1651. Purity: 98.08% by HPLC (t_R = 18.416, 19.215 min).

4.1.6.7. 2-(4-(6-chloro-7-(2-fluorophenyl)quinazolin-4-yl)piperazine-1-carbonyl)-3-phenylacrylonitrile (LLK-4). Yellow oil. Yield: 10%. ^{1}H NMR (400 MHz, $CDCl_3$) δ = 8.75 (s, 1H), 7.90 (d, J = 7.4 Hz, 2H), 7.51–7.40 (m, 5H), 7.38–7.33 (m, 1H), 7.31–7.26 (m, 1H), 7.24–7.17 (m, 1H), 7.16–7.11 (m, 1H), 6.82 (d, J = 8.8 Hz, 1H), 3.97–3.89 (m, 2H), 3.87–3.80 (m, 2H), 3.65–3.58 (m, 2H), 3.56–3.48 (m, 2H).^{13}C NMR (101 MHz, CDCl3) δ 163.38, 163.34, 153.36, 132.67, 132.02, 131.61, 131.23, 131.20, 130.84, 130.77, 130.24, 129.32, 129.29, 129.26, 124.66, 124.25, 124.21, 116.07, 115.99, 115.94, 115.72, 105.45, 49.34, 49.31. HRMS calculated for $C_{28}H_{21}ClFN_5O$ $[M+H]^+$ 498.1497. found 498.1498. Purity: 98.96% by HPLC (t_R = 17.667, 18.406 min).

4.1.6.8. 2-(4-(6-chloro-7-(2-fluorophenyl)quinazolin-4-yl)piperazine-1-carbonyl)-3-(thiophen-2-yl)acrylonitrile (LLK-5). Yellow oil. Yield: 7%. ^{1}H NMR (400 MHz, $CDCl_3$) δ = 8.78 (s, 1H), 7.97 (s, 1H), 7.93 (s, 1H), 7.59 (d, J = 5.2 Hz, 1H), 7.53 (s, 1H), 7.50–7.43 (m, 1H), 7.40–7.34 (m, 2H), 7.29 (d, J = 7.6 Hz, 1H), 7.24–7.17 (m, 1H), 7.13–7.10 (m, 1H), 3.97 (d, J = 16.6 Hz, 4H), 3.82 (s, 4H). HRMS calculated for $C_{29}H_{19}ClFN_5OS$ $[M+H]^+$ 540.1061. found 540.1058.

4.1.6.9. 2-(4-(6-chloro-7-(2-fluorophenyl)quinazolin-4-yl)piperazine-1-carbonyl)-3-(furan-2-yl)acrylonitrile(LLK-6). Yellow oil. Yield: 3%. ^{1}H NMR (400 MHz, $CDCl_3$) δ = 8.78 (s, 1H), 7.95 (d, J = 18.7 Hz, 2H), 7.58 (s, 1H), 7.51–7.44 (m, 1H), 7.41–7.34 (m, 1H), 7.29 (d, J = 7.6 Hz, 1H), 7.25–7.18 (m, 1H), 7.13 (s, 1H), 6.85 (d, J = 3.4 Hz, 1H), 6.60–6.54 (m, 1H), 3.88 (dd, J = 75.3, 16.9 Hz, 8H). MS calculated for $C_{26}H_{19}ClFN_5O_2$ $[M+H]^+$ 488.1, found 487.9.

4.1.6.10. 2-(4-(6-chloro-7-(2-fluorophenyl)quinazolin-4-yl)piperazine-1-carbonyl)-3-(pyridin-4-yl)acrylonitrile(LLK-7). Yellow oil. Yield: 5%. 1H NMR (400 MHz, $CDCl_3$) δ = 8.83–8.79 (m, 2H), 8.00 (s, 1H), 7.95 (s, 1H), 7.76 (s, 1H), 7.71 (d, J = 5.9 Hz, 2H), 7.49–7.45 (m, 1H), 7.44–7.35 (m, 2H), 7.29 (d, J = 7.3 Hz, 1H), 7.25–7.17 (m, 1H), 3.98–3.86 (m,8H). HRMS calculated for $C_{27}H_{20}ClFN_6O$ $[M+H]^+$ 499.1449. found 499.1442.

4.1.6.11. 4-(3-(4-(6-chloro-7-(2-fluorophenyl)quinazolin-4-yl)piperazin-1-yl)-2-cyano-3-oxoprop-1-en-1-yl)benzonitrile (LLK-8). Yellow oil. Yield: 5%. ^{1}H NMR (400 MHz, $CDCl_3$) δ = 8.80 (s, 1H), 8.02–7.98 (m, 3H), 7.94 (s, 1H), 7.84–7.77 (m, 3H), 7.64–7.56 (m, 1H), 7.51–7.43 (m, 1H), 7.41–7.33 (m, 1H), 7.29 (d, J = 7.5 Hz, 1H), 7.21 (t, J = 9.0 Hz, 1H), 3.93 (s, 8H).^{13}C NMR (101 MHz, $CDCl_3$). ^{13}C NMR (101 MHz, $CDCl_3$) δ 163.35, 162.15, 158.24, 154.47, 150.38, 150.30, 140.41, 135.79, 132.81, 131.81, 131.50, 131.18, 131.15, 130.77, 130.69, 130.22, 124.47, 124.19, 117.69, 116.74, 115.88, 115.67, 115.44, 115.12, 109.40, 49.23, 45.87. HRMS calculated for $C_{29}H_{20}ClFN_6O$ $[M+H]^+$ 523.1449. found 523.1443.

4.1.6.12. 2-(4-(6-chloro-7-(2-fluorophenyl)quinazolin-4-yl)piperazine-1-carbonyl)-3-(4-(trifluoromethyl)phenyl)acrylonitrile(LLK-9). Yellow oil. Yield: 10%. ^{1}H NMR (400 MHz, $CDCl_3$) δ = 8.80 (s, 1H), 8.05–7.98 (m, 3H), 7.94 (s, 1H), 7.87 (s, 1H), 7.77 (d, J = 8.2 Hz, 2H), 7.50–7.44 (m, 1H), 7.38 (t, J = 7.4 Hz, 1H), 7.29 (d, J = 7.4 Hz, 1H), 7.21 (t, J = 9.0 Hz, 1H), 3.95 (s, 8H).^{13}C NMR (101 MHz, $CDCl_3$) δ = 163.36, 162.47, 154.48, 154.41, 151.12, 150.30, 140.39, 135.07, 131.79, 131.47, 131.16, 130.75, 130.67, 130.16, 129.54, 126.17, 126.13, 124.49, 124.18, 124.15, 116.75, 115.88, 115.67, 115.34, 108.47, 49.25, 41.76. HRMS calculated for $C_{29}H_{20}ClF_4N_5O$ $[M+H]^+$ 566.1371. found 566.1374.

4.1.6.13. 1-(4-(6-chloro-7-(2-fluorophenyl)quinazolin-4-yl)piperazin-1-yl)-2-(trifluoromethyl)prop-2-en-1-one (LLK-10). Yellow oil. Yield: 10%. ^{1}H NMR (400 MHz, $CDCl_3$) δ = 8.79 (s, 1H), 7.96 (d, J = 19.2 Hz, 2H), 7.51–7.43 (m, 1H), 7.37 (t, J = 7.3 Hz, 1H), 7.29 (d, J = 7.5 Hz, 1H), 7.21 (t, J = 9.1 Hz, 1H), 6.14 (s, 1H), 5.76 (s, 1H), 4.00–3.72 (m, 8H). ^{13}C NMR (101 MHz, CDCl3) δ 163.45, 162.95, 154.45, 150.23, 140.38, 131.73, 131.47, 131.17, 131.15, 130.75, 130.67, 124.48, 124.18, 124.14, 123.18, 123.12, 116.78, 115.86, 115.65, 49.52. MS calculated for $C_{22}H_{17}ClF_4N_4O$ $[M+H]^+$ 466.1. found 466.4. Purity: 95.26% by HPLC (t_R = 17.584 min).

4.1.6.14. 6-chloro-7-(2-fluorophenyl)-4-(4-(2,2,2-trifluoroethyl)piperazin-1-yl)quinazoline (LLK-11). Yellow oil. Yield: 9%.1H NMR (400 MHz, CDCl3) δ 8.78 (s, 1H), 8.01 (s, 1H), 7.92 (s, 1H), 7.47 (t, J = 6.4 Hz, 1H), 7.39 (t, J = 7.4 Hz, 1H), 7.27–7.16 (m, 3H), 3.83–3.61 (m, 10*H*).

4.1.6.15. 3-(4-(6-chloro-7-(2-fluorophenyl)quinazolin-4-yl)piperazin-1-yl)-3-oxopropanenitrile (LLK-12). Yellow oil. Yield: 9%. 1H NMR (400 MHz, CDCl3) δ = 8.80 (s, 1H), 7.99 (s, 1H), 7.94 (s, 1H), 7.50–7.45 (m, 1H), 7.40–7.34 (m, 1H), 7.29 (d, J = 7.5 Hz, 1H), 7.21 (t, J = 9.1 Hz, 1H), 3.95–3.84 (m, 6H), 3.78–3.73 (m, 2H), 3.57 (s, 2H).MS calculated for $C_{21}H_{17}ClFN_5O$ $[M+H]^+$ 411.1. found 411.2

4.1.6.16. 1-(4-(6-chloro-7-(2-fluorophenyl)quinazolin-4-yl)piperazin-1-yl)prop-2-yn-1-one (LLK-13). Yellow oil. Yield: 5%. Purity: 95.26%.^{1}H NMR (400 MHz, $CDCl_3$) δ = 8.79 (s, 1H), 7.99 (s, 1H), 7.93 (s, 1H), 7.50–7.44 (m, 1H), 7.40–7.34 (m, 1H), 7.29 (d, J = 7.4 Hz, 1H), 7.21 (t, J = 9.1 Hz, 1H), 4.05–3.98 (m, 2H), 3.92–3.86 (m, 4H), 3.85–3.80 (m, 2H), 3.00 (s, 1H).^{13}C NMR (101 MHz, $CDCl_3$) δ165.91, 163.66, 163.32, 154.45, 140.34, 133.11, 131.70, 131.60, 131.37, 131.19, 131.16, 130.74, 130.66, 124.55, 124.17, 124.14, 115.88, 115.66, 52.21, 49.66, 49.22, 45.47, 41.82. HRMS calculated for $C_{21}H_{16}ClFN_4O$ $[M+H]^+$ 395.1080. found 395.1081. Purity: 95.12% by HPLC (t_R = 16.411 min).

4.1.6.17. Methyl-4-(4-(6-chloro-7-(2-fluorophenyl)quinazolin-4-yl)piperazin-1-yl)-4-oxobut-2-enoate (LLK-14). Yellow oil. Yield: 7%. Purity: 95.12%. ^{1}H NMR (400 MHz, $CDCl_3$) δ = 8.79 (s, 1H), 7.99 (s, 1H), 7.93 (s, 1H), 7.51–7.42 (m, 2H), 7.40–7.33 (m, 1H), 7.29 (d, J = 7.5 Hz, 1H), 7.21 (t, J = 9.0 Hz, 1H), 6.86 (d, J = 15.3 Hz, 1H), 3.97–3.91 (m, 2H), 3.90–3.84 (m, 6H), 3.83 (s, 3H).^{13}C NMR (101 MHz, $CDCl_3$) δ163.42, 154.45, 152.00, 140.38, 131.72, 131.44, 131.19, 131.16, 130.75, 130.67, 124.52, 124.18, 116.75, 115.88, 115.66, 79.90, 75.03, 49.67, 49.27, 46.42, 41.21. HRMS calculated for $C_{23}H_{19}ClFN_5O$ $[M+H]^+$ 436.0838. found 436.0839.

4.2. Cell culture and cytotoxicity assay

The antiproliferative activity of all compounds was evaluated against the human pancreatic cancer cell line miapanc2, panc1, human lung cancer cell line H358, A549 and human breast cancer cells line MCF7 by using the standard MTT assay *in vitro*, with ARS-1620 as the positive control. All the cancer cell lines were cultured in DMEM medium supplemented with 10% fetal bovine serum (FBS). Cells were seeded into 96-well plates at a density of 5×10^3 cells/well and then treated with 0.1% DMSO, ARS-1620 or test compounds for 24 h.100 μL of MTT was added to each well, and incubated with cells at 37 °C for 4 h. The formazan crystals were dissolved in 100 mL DMSO each well, and the absorbency at 490 nm (for absorbance of MTT formazan). All of the compounds were tested three times in each of the cell lines. The IC_{50} (inhibitory concentration 50%) value were presented as mean ± standard deviation (SD).

4.3. Mass spectrometry analysis (MS)

RAS G12C protein was treated with DMSO or a 10-fold molar excess of compound **LLK10** for 2 h at room temperature. Reactions were directly analyzed by LC-MS.

4.4. ITC and CD analysis

All the proteins were obtained from commercial source: KRAS G12C (Cat No:CR63) The ITC experiment was performed using a MicroCal PEAQ-ITC (Malvern Panalytical Ltd., UK), ITC experiments were performed according to the manufacturer's guidelines. CD spectra were recorded on a Chirascan plus ACD (Applied Photophysics Ltd, England). Briefly, KRAS G12C protein were incubated with sterile water or **LLK-10** at 25 °C for 30 min, the CD wave scans were measured from 180 to 260 nm at 4 °C with the band width of 2 nm and the step size of 1 nm.

4.5. Immunoblotting

Cells were washed once with 1x phosphate buffered saline (PBS) and then lysed in RIPA buffer supplemented with protease and phosphatase inhibitors. Protein concentrations were determined by using the Pierce BCA protein assay kit. Equal amount of protein was resolved on SDS-PAGE, and was subsequently transferred onto nitrocellulose membrane. The membrane was blocked with 5%non-fat milk in TBST and was then incubated with primary antibodies overnight at 4 °C with gentle rotating. After washing, the membrane was incubated with secondary antibodies for 1 hr at room temperature. The membrane was then washed and scanned with an Odyssey Infrared scanner (Li-Cor Biosciences). Primary antibodies include anti-KRAS(Cell Signaling Technology #SAB1404011), anti-phospho-p44/42 MAPK (Erk1/2) (Cell Signaling Technology # 9101S), anti- p44/42 MAPK (Erk1/2) (Abacam #ab178876), anti-phospho-MEK1/2 (Ser217/221) (Cell Signaling Technology # 9154P), anti-MEK1/2 (abacam #ab178876), and anti-Tubulin (Cell Signaling Technology # 3873S).

4.6. Colony formation assay

H358 cells (1000 units) were counted and seeded in 6-wells plates for colony formation assay. Cells were cultured for 24 h at 37 °C and then the media were replaced with media added with **LLK-10** at the indicated concentration. After 24 h treatment, the media were changed to normal and cells were cultured for 7 days. The colonies were fixed with 4% paraformaldehyde for 30 min and stained with 0.1% Crystal Violet for 15 min and washed. The colonies were then photographed and counted

by the Image J.

4.7. Molecular modeling

The molecular modeling studies were performed with Schrodinger Molecular Modeling Suite 2011 (Schrodinger LLC, New York, NY) running on a Philips window workstation. The crystal structure of KRAS G12C complexed with ARS 1620 (PDB:5V9U) was retrieved from the RCSB Protein Data Bank (http://www.rcsb.Org/pdb). **ARS-1620** and **LLK10** was prepared using the Ligprep module, and they were docked into the SWII site by the covalent docking protocol in the Schrodinger Suite.

Declaration of Competing Interest

The authors declare that they have no known competing financial interests or personal relationships that could have appeared to influence the work reported in this paper.

Acknowledgement

This work was supported by scientific research project of high level talents (No. C1051008) in Southern Medical University of China; Thousand Youth Talents Program (No. C1080092) from the Organization Department of the CPC Central Committee, China; and International Science and Technology Cooperation Projects of Guangdong Province (No. G819310411).

Appendix A. Supplementary material

Supplementary data to this article can be found online at https://doi.org/10.1016/j.bioorg.2021.104825.

References

[1] D.K. Simanshu, D.V. Nissley, F. McCormick, RAS proteins and their regulators in human disease, Cell 170 (2017) 17–33, https://doi.org/10.1016/j.cell.2017.06.009.
[2] D. Uprety, A.A. Adjei, KRAS: From undruggable to a druggable Cancer Target, Cancer Treat. Rev. 89 (2020) 102070, https://doi.org/10.1016/j.ctrv.2020.102070.
[3] J.G. Christensen, P. Olson, T. Briere, C. Wiel, M.O. Bergo, Targeting Krasg12c-mutant cancer with a mutation-specific inhibitor, J. Intern. Med. 288 (2020) 183–191, https://doi.org/10.1111/joim.v288.210.1111/joim.13057.
[4] A.D. Cox, S.W. Fesik, A.C. Kimmelman, J.i. Luo, C.J. Der, Drugging the undruggable RAS: Mission Possible? Nat. Rev. Drug Discovery 13 (2014) 828–851, https://doi.org/10.1038/nrd4389.
[5] H. Adderley, F.H. Blackhall, C.R. Lindsay, KRAS-mutant non-small cell lung cancer: Converging small molecules and immune checkpoint inhibition, EBioMedicine 41 (2019) 711–716, https://doi.org/10.1016/j.ebiom.2019.02.049.
[6] A. Mullard, K.R.A.S. Cracking, Nat. Rev. Drug Discovery 18 (2019) 887–891, https://doi.org/10.1038/d41573-019-00195-5.
[7] Y. Wang, C.E. Kaiser, B. Frett, H.-y. Li, Targeting mutant KRAS for anticancer therapeutics: a review of novel small molecule modulators, J. Med. Chem. 56 (2013) 5219–5230, https://doi.org/10.1021/jm3017706.
[8] J.M. Ostrem, U. Peters, M.L. Sos, J.A. Wells, K.M. Shokat, K-Ras(G12C) inhibitors allosterically control GTP affinity and effector interactions, Nature 503 (2013) 548–551, https://doi.org/10.1038/nature12796.
[9] M.R. Janes, J. Zhang, L.-S. Li, R. Hansen, U. Peters, X. Guo, Y. Chen, A. Babbar, S. J. Firdaus, L. Darjania, J. Feng, J.H. Chen, S. Li, S. Li, Y.O. Long, C. Thach, Y. Liu, A. Zarieh, T. Ely, J.M. Kucharski, L.V. Kessler, T. Wu, K.e. Yu, Y.i. Wang, Y. Yao, X. Deng, P.P. Zarrinkar, D. Brehmer, D. Dhanak, M.V. Lorenzi, D. Hu-Lowe, M. P. Patricelli, P. Ren, Y.i. Liu, Targeting KRAS mutant cancers with a covalent G12C-specific inhibitor, Cell 172 (2018) 578–589.e17, https://doi.org/10.1016/j.cell.2018.01.006.
[10] C.-U. Lee, T.N. Grossmann, Reversible covalent inhibition of a protein target, Angew. Chem. Int. Ed. 51 (2012) 8699–8700, https://doi.org/10.1002/anie.v51.3510.1002/anie.201203341.
[11] S.E. Salmon, Human tumor clonogenic assays: growth conditions and applications, Cancer Genet Cytogene. 19 (1986) 21–28, https://doi.org/10.1016/0165-4608(86)90367-5.